

Optical Engineering

OpticalEngineering.SPIEDigitalLibrary.org

Incoherent optical generalized Hough transform: pattern recognition and feature extraction applications

Ariel Fernández
José A. Ferrari

SPIE.

Ariel Fernández, José A. Ferrari, "Incoherent optical generalized Hough transform: pattern recognition and feature extraction applications," *Opt. Eng.* **56**(5), 053107 (2017), doi: 10.1117/1.OE.56.5.053107.

Incoherent optical generalized Hough transform: pattern recognition and feature extraction applications

Ariel Fernández* and José A. Ferrari

Universidad de la República, Instituto de Física, Facultad de Ingeniería, Montevideo, Uruguay

Abstract. Pattern recognition and feature extraction are image processing applications of great interest in defect inspection and robot vision among others. In comparison to purely digital methods, the attractiveness of optical processors for pattern recognition lies in their highly parallel operation and real-time processing capability. This work presents an optical implementation of the generalized Hough transform (GHT), a well-established technique for recognition of geometrical features in binary images. Detection of a geometric feature under the GHT is accomplished by mapping the original image to an accumulator space; the large computational requirements for this mapping make the optical implementation an attractive alternative to digital-only methods. We explore an optical setup where the transformation is obtained, and the size and orientation parameters can be controlled, allowing for dynamic scale and orientation-variant pattern recognition. A compact system for the above purposes results from the use of an electrically tunable lens for scale control and a pupil mask implemented on a high-contrast spatial light modulator for orientation/shape variation of the template. Real-time can also be achieved. In addition, by thresholding of the GHT and optically inverse transforming, the previously detected features of interest can be extracted. © 2017 Society of Photo-Optical Instrumentation Engineers (SPIE) [DOI: 10.1117/1.OE.56.5.053107]

Keywords: Hough transform; analog optical image processing; pattern recognition; feature extraction.

Paper 170342P received Mar. 9, 2017; accepted for publication Apr. 27, 2017; published online May 16, 2017.

1 Introduction

One of the most important tasks in automated image analysis is the recognition of geometric features. In particular the Hough transform (HT)¹ is a well-known algorithm for line detection in edge binary images and has been established in recent decades^{2–4} as a robust pattern recognition technique, capable of handling disconnected boundaries, or noise in the input image. It has also been extended to other parametric curves such as circles (circular Hough transform) or ellipses and has been successfully applied in motion detection, biometric authentication, medical imaging, and robot navigation among others.

An extension of the HT algorithm known as generalized Hough transform (GHT)^{5,6} allows for the detection of more complex patterns with no analytical representation. The GHT has proven to be useful, for example, in automated satellite imagery navigation,⁷ medical imaging,⁸ identification of chips⁹ or tag devices¹⁰ in assembly lines and fingerprint recognition.¹¹

Image processing transforms can benefit from real-time and parallel processing enabled by optics. Optical architectures for the HT have been proposed in the literature,^{12,13} mostly working under coherent illumination. With the capability of achieving signals with less speckle noise, the use of incoherent illumination was also suggested for the HT by Steier and Shori¹² and Schmid et al.¹⁴

Coherent approaches for the optical implementation of the GHT can be found in the literature. The use of lasers acousto-optically modulated and the piecewise representation of the template through analytical curves was proposed by Casasent and Richards.¹⁵ Javadpour and Keating¹⁶ generalized the method presented by Seth and Datta¹⁷ to handle nonanalytical shapes by considering a look-up table that

defines the shape and also speeded up the basic configuration introducing an acousto-optical implementation of the matrix-vector multiplication. The use of a matrix of holograms was proposed by Shin and Jang,¹⁸ where the scale and rotation-variant detection are accomplished by spatial multiplexing.

Fernández et al.¹⁹ recently proposed an incoherent correlator for the optical implementation of the GHT. This processor is based on the point-spread function of a highly blurred optical system in which the focal setting along with the pupil orientation can be efficiently controlled. In Sec. 2 a compact optical setup resulting from the use of an electrically tunable lens for scale control and a rotating pupil mask (implemented on a high-contrast spatial light modulator [SLM]) for orientation variation is presented.

The pattern recognition capability of the optical processor is addressed in Sec. 3 where, based on the previous setup, temporal multiplexing schemes for the recognition of geometrical features of different size and shape/orientation²⁰ are implemented.

Finally, in Sec. 4 extraction of a given feature after detection is addressed by thresholding of the GHT and optical inverse transforming.²¹

2 Generalized Hough Transform

Let us start by considering a binary edge image $I(x, y)$ and a template defined by the constraint equation

$$f(x, y; s, \theta) = 0, \quad (1)$$

where s is the (isotropic) scale parameter and θ is the orientation of the shape (Fig. 1).

*Address all correspondence to: Ariel Fernández, E-mail: arielfer@fing.edu.uy

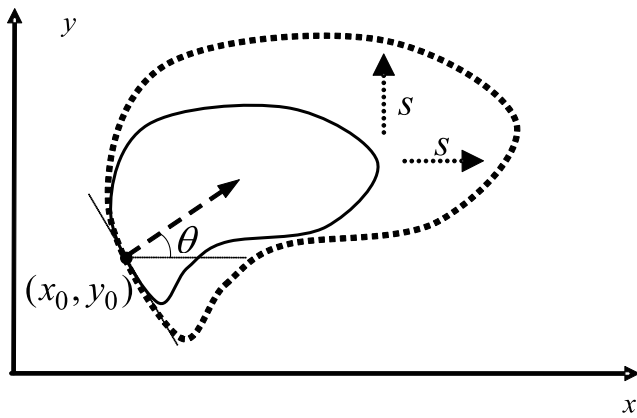


Fig. 1 Parameters for an arbitrary shape.

The GHT can be written as¹⁹

$$H(x, y; s, \theta) = \int_{-\infty}^{+\infty} \int_{-\infty}^{+\infty} I(x', y') \delta[f(x' - x, y' - y; s, \theta)] dx' dy'. \quad (2)$$

The close connection between the recognition of an arbitrary shape and template matching algorithm was pointed out by Merlin and Farber²² and Sklansky;²³ it is clear that the integral representation of the GHT of a binary image $I(x, y)$ given by Eq. (2) corresponds to a correlation, whose kernel is given by the Dirac delta function $\delta[f(x, y; s, \theta)]$. In order to proceed into the optical implementation of the GHT, let us consider a π rotation of the template, whose constraint equation is

$$f_{\pi}(x, y; s, \theta) = f(-x, -y; s, \theta), \quad (3)$$

so we can rewrite Eq. (2) as

$$H(x, y; s, \theta) = \int_{-\infty}^{+\infty} \int_{-\infty}^{+\infty} I(x', y') \delta[f_{\pi}(x - x', y - y'; s, \theta)] dx' dy', \quad (4)$$

which is exactly in the form of a convolution between the image $I(x, y)$ and the π -rotated template. Consider for example, the binary image in Fig. 2(a) and its GHT in Fig. 2(b) using as a template the rotated triangle of the inset. The GHT exhibits a clear maximum at the center of the triangle in Fig. 2(a), which corresponds to exact matching to the template.

2.1 Optical Implementation of the GHT

The convolution form in Eq. (4) is suitable for an optical implementation in systems that are linear in the intensity of the input. To achieve an optical implementation of the GHT, we need a system whose point spread function (PSF) is given by $\delta[f_{\pi}(x, y; s, \theta)]$. A physically reasonable approximation to the desired PSF can be achieved by means of a severely defocused optical system (that is, a system where the dominant aberration is defocus)²⁴ with a pupil whose transmittance is different from zero only along the desired curve, since in a severely defocused incoherent system the PSF is essentially the geometrical projection of the pupil onto the output plane.²⁵

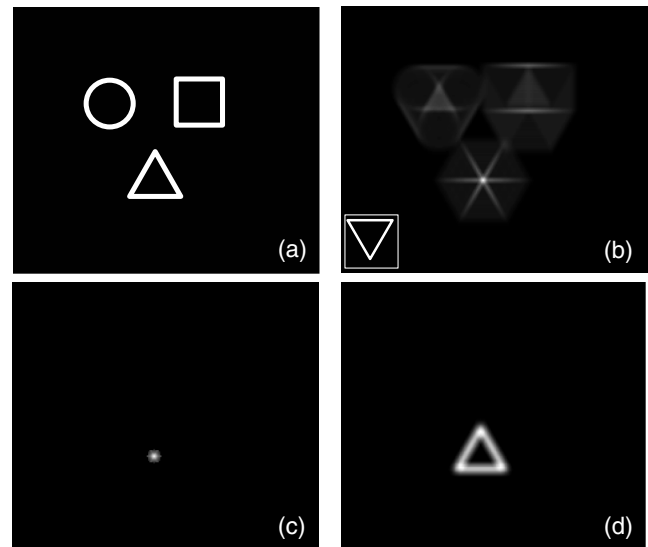


Fig. 2 GHT and feature extraction. (a) Edge-enhanced binary image I (the feature of interest is the triangle); (b) GHT of (a) using the template in the lower left corner inset; (c) thresholding of (b); (d) result obtained after inverse filtering of (c).

In order to obtain the desired PSF, we proposed the setup shown in Fig. 3. The edge image to be processed (which contains the shape we are looking for along with other shapes) is displayed in the object plane O and is illuminated by a totally (both temporal and spatial) incoherent source. The imaging lens system (L) is placed at distance d_1 from O . The template (shape of interest) is set as the pupil (P) of the lens system and consists of a nontransparent mask (P) with significant light transmission only across a thin curve emulating the desired edge template. The GHT is obtained on the plane C at distance d_c from L .

As an example of the working principle, consider Fig. 4 where the GHT of a three-point image is optically achieved. The triangle whose vertices are these points is overlaid at the object plane while its (in-focus) image is overlaid at the capture plane; note that in a single thin lens system the in-focus image is inverted with respect to the object itself. As the

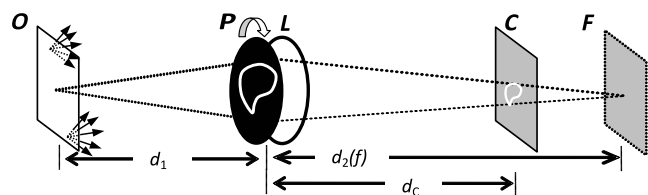


Fig. 3 Optical implementation of the GHT on plane C . O , object plane; P , binary pupil mask; L , imaging system (focal distance f); F , in-focus plane at distance $d_2(f)$ from imaging system.



Fig. 4 Optical implementation of the GHT with triangular pupil following the configuration of Fig. 3.

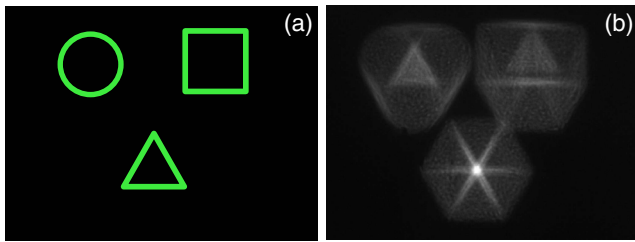


Fig. 5 (a) Original image; (b) GHT of (a) using a triangular pupil, as captured on camera [note the close resemblance to the simulation in Fig. 2(b)].

capture plane C lies before the in-focus plane F [i.e., $d_C \leq d_2(f)$ in Fig. 3], the geometrical projection of the pupil is not inverted with respect to the pupil itself, so it appears inverted with respect to the in-focus object over which the GHT is to be applied.

In our experimental setup, an LED-illuminated liquid crystal display is used for displaying the binary images in the object plane. The desired template with its corresponding orientation θ (mask P in Fig. 3) is displayed on an SLM (Holoeye LC2002, 600×800 pixels). The imaging system L is an electrical tunable lens (ETL) with controllable focal length f (Optotune, EL-10-C, focal length 210 to 80 mm for currents 0 to 300 mA). The effective size of the projection of the pupil on the C -plane increases as $d_2(f)$ increases (i.e., F moves away from L) so we can control the scale parameter s by varying the focal distance f .

3 Pattern Recognition with the Incoherent GHT

It is expected from a pattern-recognition device to be able to recognize any given template, regardless of its position in the image, its orientation or its size or scale of magnification.²⁶ The setup previously presented allows for robust,²⁷ real-time²⁰ pattern recognition with variable orientation/shape or scale under suitable time-multiplexing strategies.

3.1 Shape-Variant Detection

Consider for example Fig. 5(a) where we want to detect a triangle out of figures of different shapes and similar sizes. A bright spot is found at the center of the matching object (in this case the pupil is a triangle) as shown in Fig. 5(b).

3.2 Scale-Variant Detection

Figure 6(a) shows an image of three binary circles in which we want to detect a circle of specific radius (and rule out those with different radii) by applying the optical GHT. The results of transforming the image for different scale parameters (radii) are shown in Figs. 6(b)–6(d). It can also be clearly seen that the GHT exhibits an intensity peak at the center of the circle whose radius coincides with the radius R of the projected pupil, which in turn can be varied by changing the focal length f of the ETL.

4 Feature Extraction

For the feature extraction, peaks in the transformation need to be mapped back to image space. However, these peaks represent the most voted parameter combinations but not the pixels that gave rise to them. In order to recover the pixels related to the most voted parameter combination, we need to

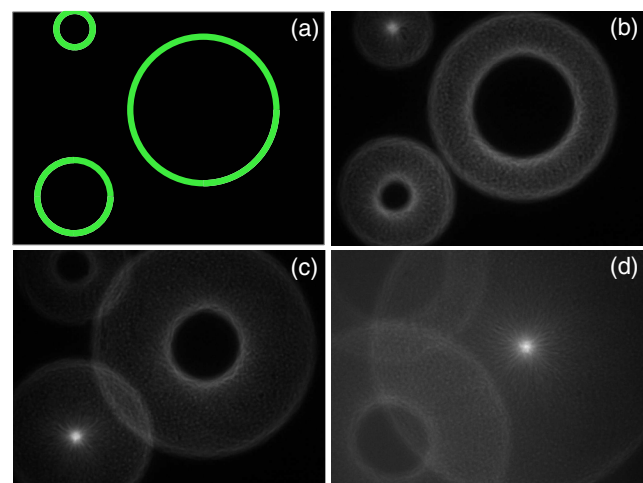


Fig. 6 Recognition of a circle of given radius R in an image of three binary circles of radius R_1 , $R_2 = 2R_1$, and $R_3 = 4R_1$. (a) Original image; (b–d) optical GHT on the plane C (as captured on camera, no postprocessing). Bright points mark the center of the circle in original image with $R = R_1$, R_2 and R_3 , respectively.

proceed through thresholding [Fig. 2(c)] followed by inverse transforming [Fig. 2(d)]. The key point for the optical implementation of this procedure lies in the fact that, apart from magnification and inversion, geometrical optics predicts that at in-focus plane [at distance $d_2(f)$ in Fig. 3] we recover the original image, as can be seen in the capture at C_2 in Fig. 7(a). That is, since at distance d_C we obtain the GHT [Eq. (4)] of the input image I

$$H(I), \quad (5)$$

in order to recover the input at $d_2(f)$, inverse GHT (H^{-1}) is performed between d_C and $d_2(f)$

$$H^{-1}[H(I)] = I, \quad (6)$$

which naturally results in the object itself. If we instead place at d_C , a thresholded version of $H(I)$: $Th[H(I)]$ where we retain only the intensity values above a certain threshold (typically 90% to 95% of the peak value of the transformation), inversion will be performed only on these points

$$H^{-1}\{Th[H(I)]\}, \quad (7)$$

and we can expect to find at the in-focus plane just the part of the input image giving rise to the peak in the GHT [capture at C_2 in Fig. 7(b)], that is, the part of the input in exact matching to the template.

The setup to perform the GHT followed by thresholding and inversion (Fig. 7) consists of an object plane O where a binary image containing the shape we are looking for—along with other shapes—is displayed. By means of a beam splitter (BS), the same GHT is simultaneously imaging at C_1 (where a camera is placed and used to acquire a digital image of the transformation) and SLM planes. Thresholding of the GHT at SLM is performed using the information from C_1 . In order to filter the maxima of the GHT, a binary mask is set at the SLM plane: for those pixels with intensity values in the camera C_1 above a certain threshold (typically 90% to 95% of I_{\max}), the transmittance of the corresponding pixels in SLM

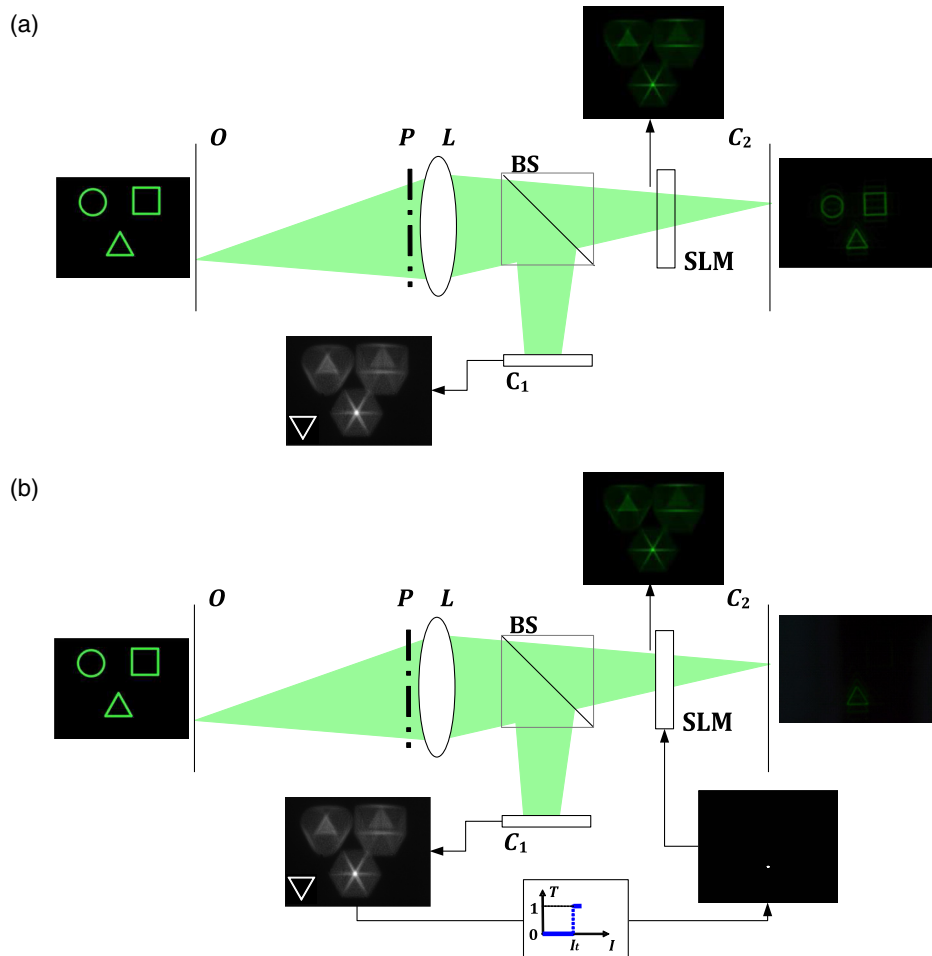


Fig. 7 Experimental setup for optical GHT with nonlinear filtering. O, object plane; P, pupil; L, lens system; BS, beam-splitter; SLM, spatial light modulator; C_{1,2}, capture planes. Transmittance (T) of the pixels in the SLM is set to (a) one for all pixels (b) one for those pixels corresponding to intensity I in the GHT at C_1 above threshold I_t (and zero for the rest). For clarity, GHT's and captures are shown with no inversion with respect to input.

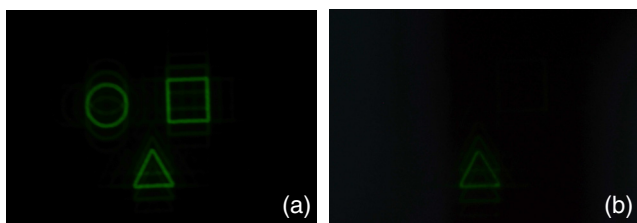


Fig. 8 Feature extraction by shape. (a) Capture at image plane C_2 under full transmittance of SLM; (b) capture at the image plane C_2 after filtering.

is set to unit and zero for the rest. Given that inverse transforming is performed between GHT and in-focus planes (where SLM and C_2 are placed, respectively), we are able to capture at C_2 only the information corresponding to the template we are looking for in the original image. Results for feature extraction by shape are shown in Fig. 8 (feature extraction by orientation or shape works in a similar way).

5 Conclusions

We have demonstrated that it is possible to achieve shape and scale-variant pattern recognition (based on the GHT) in an

incoherent optical setup. Through the simultaneous imaging and nonlinear filtering of the GHT, feature extraction can also be performed. All-optical image processing (from edge detection to feature extraction) is a promising future line of work that can arise from the combination of incoherent edge-enhancement^{28–30} and incoherent correlation and optical feature extraction as presented in this work.

Acknowledgments

We acknowledge financial funding from Programa de Desarrollo de las Ciencias Básicas (PEDECIBA, Uruguay) and Comisión Sectorial de Investigación Científica (CSIC, UdelaR, Uruguay). A significant part of this paper was presented at *Optics and Photonics for Information Processing X*.³¹

References

1. R. O. Duda and P. E. Hart, "Use of the Hough transformation to detect lines and curves in pictures," *Commun. ACM* **15**(1), 11–15 (1972).
2. P. Mukhopadhyay and B. B. Chaudhuri, "A survey of Hough transform," *Pattern Recognit.* **48**(3), 993–1010 (2015).
3. V. Leavers, "Which Hough transform?" *CVGIP Image Understanding* **58**(2), 250–264 (1993).
4. J. Illingworth and J. Kittler, "A survey of the Hough transform," *Comput. Vision Graphics Image Process.* **44**(1), 87–116 (1988).

5. D. H. Ballard, "Generalizing the Hough transform to detect arbitrary shapes," *Pattern Recognit.* **13**(2), 111–122 (1981).
6. C. L. L. Hendriks et al., "The generalized radon transform: sampling, accuracy and memory considerations," *Pattern Recognit.* **38**(12), 2494–2505 (2005).
7. B. Chen and X. Deng, "A landmark matching algorithm using the improved generalised Hough transform," *Proc. SPIE* **9643**, 96431V (2015).
8. G. Ricca, M. C. Beltrametti, and A. M. Massone, "Piecewise recognition of bone skeleton profiles via an iterative Hough transform approach without re-voting," *Proc. SPIE* **9413**, 94132M (2015).
9. M. Ulrich, C. Steger, and A. Baumgartner, "Real-time object recognition using a modified generalized Hough transform," *Pattern Recognit.* **36**(11), 2557–2570 (2003).
10. H. Yang et al., "Polygon-invariant generalized Hough transform for high-speed vision-based positioning," *IEEE Trans. Autom. Sci. Eng.* **13**(3), 1367–1384 (2016).
11. J. Qi et al., "A novel fingerprint matching method based on the Hough transform without quantization of the Hough space," in *Third Int. Conf. on Image and Graphics (ICIG '04)*, pp. 262–265, IEEE (2004).
12. W. H. Steier and R. K. Shori, "Optical Hough transform," *Appl. Opt.* **25**(16), 2734–2738 (1986).
13. P. Ambs et al., "Optical implementation of the Hough transform by a matrix of holograms," *Appl. Opt.* **25**(22), 4039–4045 (1986).
14. V. R. Schmid, G. Bader, and E. H. Lueder, "Shift-, rotation-, and scale-invariant shape recognition system using an optical Hough transform," *Proc. SPIE* **3306**, 102–112 (1998).
15. D. Casasent and J. Richards, "High-speed acousto-optic mapping modulator for the generalized Hough transform," *Appl. Opt.* **32**(35), 7217–7224 (1993).
16. Z. Javadvpour and J. G. Keating, "Connectionist model of the generalized Hough transform for optical implementation," *Opt. Eng.* **39**(6), 1717–1722 (2000).
17. M. Seth and A. K. Datta, "Optical implementation of a connectionist model of Hough transform," *Opt. Eng.* **35**(6), 1779–1784 (1996).
18. D.-H. Shin and J.-S. Jang, "Optical implementation of the generalized Hough transform by use of multiplexed holograms," *Opt. Eng.* **39**(9), 2431–2438 (2000).
19. A. Fernández et al., "Optical implementation of the generalized Hough transform with totally incoherent light," *Opt. Lett.* **40**(16), 3901–3904 (2015).
20. A. Fernández et al., "Real-time pattern recognition using an optical generalized Hough transform," *Appl. Opt.* **54**(36), 10586 (2015).
21. A. Fernández et al., "Image segmentation by nonlinear filtering of optical Hough transform," *Appl. Opt.* **55**(13), 3632–3638 (2016).
22. P. M. Merlin and D. J. Farber, "A parallel mechanism for detecting curves in pictures," *IEEE Trans. Comput. C-24(1), 96–98 (1975).*
23. J. Sklansky, "On the Hough technique for curve detection," *IEEE Trans. Comput. C-27*, 923–926 (1978).
24. V. N. Mahajan and J. A. Díaz, "Comparison of geometrical and diffraction imaging in the space and frequency domains," *Appl. Opt.* **55**(12), 3241–3250 (2016).
25. J. W. Goodman, *Introduction to Fourier Optics*, McGraw-Hill, New York (1996).
26. P. Bone, R. Young, and C. Chatwin, "Position-, rotation-, scale-, and orientation-invariant multiple object recognition from cluttered scenes," *Opt. Eng.* **45**(7), 077203 (2006).
27. A. Fernández, "Robust pattern recognition with optical generalized Hough transform," in *Imaging Systems and Applications*, JTU3A–58 (2016).
28. A. Fernández et al., "Optical processing of color images with incoherent illumination: orientation-selective edge enhancement using a modified liquid-crystal display," *Opt. Express* **19**(21), 21091 (2011).
29. J. L. Flores et al., "Analog image contouring using a twisted-nematic liquid-crystal display," *Opt. Express* **18**(18), 19163 (2010).
30. J. L. Flores et al., "Incoherent optical processor for nondirectional edge enhancement of color images," *Opt. Lett.* **36**(23), 4596–4598 (2011).
31. A. Fernández, "Pattern recognition and feature extraction with an optical Hough transform," *Proc. SPIE* **9970**, 99700N (2016).

Ariel Fernández is an assistant at the Engineering Faculty of the Universidad de la República, Uruguay. He received his MA and PhD degrees in physics from this university. His areas of research are in applied optics, in particular in image processing by optical methods, pattern recognition, and Fourier optics. He is a member of SPIE.

José A. Ferrari is a professor at the Engineering Faculty of the Universidad de la República, Uruguay. He received his PhD in physics from the Technische Universität Berlin. His areas of research are applied optics, in particular in image processing by optical methods, Fourier optics, and interferometry. He is a member of SPIE.